Supporting Information

Sensitive and Site-Selective Determination of Phosphorylated Peptides with a Ratiometric Photoelectrochemical Strategy

Baihe Fu, Zhonghai Zhang*

Shanghai Key Laboratory of Green Chemistry and Chemical Processes, School of Chemistry and Molecular Engineering, East China Normal University, Shanghai 200241, China

Address correspondence to zhzhang@chem.ecnu.edu.cn

I. Experimental Section

Chemicals and materials
Preparation of TiO_2 nanowires (r-TiO_2 NWs) and TiO_2 nanotubes(a-TiO_2 NTs)
Materials Characterization
Photoelectrochemical measurements
Real samples detection

II. Additional Figure S1-S10

Figure S1. Diffuse reflectance spectra of absorbance of (a) r-TiO_2 NWs and (b) a-TiO_2 NTs.
Figure S2. Raman spectra of (a) r-TiO_2 NWs and (b) a-TiO_2 NTs.
Figure S3. (a) Top-view SEM image; (b) TEM image; (c) cross-sectional SEM image; (d) high magnification of cross-sectional SEM image; closer observation of high resolution of top-view SEM image.
Figure S4. (a) Top-view SEM image; (b-d) TEM images; (e) cross-sectional SEM image.
Figure S5. FTIR spectroscopy of (a) r-TiO_2 NWs, peptide/r-TiO_2 NWs, phosphopeptide/r-TiO_2 NWs; (b) a-TiO_2 NTs, peptide/a-TiO_2 NTs, phosphopeptide/a-TiO_2 NTs.
Figure S6. Amperometric transient photocurrent vs time plots of (a) r-TiO_2 NWs and (b) a-TiO_2 NTs at applied potential of 0.5 V vs Ag/AgCl under illumination of simulated solar light with different concentrations of phosphopeptides.
Figure S7. PEC responses of (a1) BSA, (a2) human serum, and (a3) skim milk on r-TiO2 NWs, and of (b1) BSA, (b2) human serum, and (b3) skim milk on a-TiO2 NTs.
Figure S8. XPS survey of nonphosphopeptide/r-TiO_2 NWs.
Figure S9. Core-level XPS of N 1s on phosphopeptide/r-TiO_2 NWs.
Figure S10. (a) Electrochemical impedance spectra of Nyquist plots of a-TiO_2 NTs and phosphopeptide/a-TiO_2 NTs, (b) Mott-Schottky plots of a-TiO_2 NTs and phosphopeptide/a-TiO_2 NTs.

III. Additional References

I. Experimental Section

Chemicals and Materials. Fluorine-doped-tin-oxide (FTO) glass (50 × 10 mm^2) was supplied from Kaivo Optoelectronic Technology Co., Ltd, Zhuhai, China. The thickness of titanium foil was 0.1 mm (99.6%, Jinjia Metal, China). Hydrochloric (HCl), isopropyl titanate, acetic acid, acetic sodium, ethylene glycol (EG) and ammonia fluoride (NH4F) were purchased from Macklin Chemical and used as received. The peptides were synthesized and purified by ChinaPeptides Co., Ltd. (Shanghai, China). The sequences are listed below:

Phosphopeptide: GG(p-S)GGTGGY, GGSGG(p-T)GGY, GGSGGTGG(p-Y), D(p-S)GEGDFLAEGGGVR

Nonphosphopeptide: GGSGGTGGY, DSGEGDFLAEGGGVR

All aqueous solutions were prepared using deionized water (DI) with a resistivity of 18.2 MΩ cm.

Preparation of TiO_2 nanowires. The synthesis of FTO-TiO_2 nanowires was carried out in a 25 mL Teflon-lined stainless steel autoclave. In a typical procedure, 10 mL HCl were dissolved in 10 mL DI water. After stirring for 10 min, 0.5 mL of isopropyl titanate were added into the mixture. The mixture was transferred into the Teflon-lined stainless steel autoclave and maintained at 150 °C for 12 h. Finally, the autoclave was cooled down to room temperature. The FTO glass was covered with white TiO_2 nanowires and washed with DI water for several times. The as-prepared TiO_2 nanowires were annealed in air at 500 °C for 1 h to increase the degree of crystallinity.

Preparation of TiO_2 nanotubes. The TiO_2 nanotubes were fabricated by a two-step anodization process. Prior to anodization, the Ti foils were first degreased by sonicating orderly in acetone, ethanol and DI water, followed by drying in pure nitrogen stream. The anodization was carried out using a conventional two-electrode system with the Ti foil as an anode and a Pt foil as a cathode respectively. All electrolytes consisted of 0.32 wt% NH_4F in EG solution with 2.7 vol% water. All the anodization was carried out in room temperature. In the anodization, the Ti foil was first anodized at 60 V for 0.5 h, and then the as-grown nanotube layer was ultrasonically removed in deionized water. Then after drying in pure nitrogen, the Ti foil was second anodized at 30 V for 0.5 h. The as-prepared TiO_2 nanotube samples were cleaned with DI water and dried off with nitrogen gas. The as-prepared TiO_2 nanotubes were annealed in air at 500 °C for 1 h to increase the degree of crystallinity.

Material Characterizations. The microscopic morphologies of photoelectrode were characterized by scanning electron microscopy (SEM; Hitachi S4800) and high resolution transmission electron microscopy (HRTEM, JEOL JEM 2100). The crystalline structure was analyzed by X-ray diffraction (XRD) (Bruker D8 Discover diffractometer, using Cu Kα radiation (1.540598 Å)). Selective adsorption of phosphopeptide was measured from Fourier transform infrared (FTIR) spectroscopy (Nicolet, S50) and X-ray photoelectron spectroscopy (XPS, Kratos Analytical). The diffuse reflectance UV-vis adsorption spectra were recorded on a spectrophotometer (Shimadazu, UV 3600), with fine $BaSO_4$ powder as reference. The Raman spectra were measured through DXR Raman Microscope (Thermo).

Photoelectrochemical measurements. All the photoelectrochemical measurements were performed with CHI 660E electrochemical working station in a three-electrode system with r-TiO_2 NWs and a-TiO_2 NTs electrode as working electrode, a platinum foil as the counter electrode, and Ag/AgCl with saturated KCl solution as the reference electrode. Before measurements, the TiO_2 photoelectrodes were incubated in phosphopeptide and nonphosphopeptide solution at 37 °C for 30 min. The supporting electrolyte was HAc-NaAc (pH = 6.2) solution. The transient photoresponse was evaluated under simulated sunlight irradiation (light on/off cycles: 60 s) at a fixed electrode potential of 0.5 V vs Ag/AgCl. The electrochemical impedance spectra (EIS) were measured using a PGSTAT 302N Autolab Potentiostat/Galvanostat (Metrohm) equipped with a frequency-analyzer module (FRA2) with an excitation signal of 10 mV amplitude. Lighting apparatus used in the experiment is simulated solar light irradiation (100 mW cm^{-2}) (PLS-sxe300).

Real samples detection. Bovine serum albumin (BSA) were dissolved in a solution of ammonium bicarbonate (50 mM, pH ~ 10) with a final concentration of 20 μg μL^{-1}, followed by digestion with trypsin. The mixture with a concentration ratio of 50:1 (protein versus trypsin) was incubated in a 37 °C water bath for 24 h. For skim milk, 30 μL of the sample was diluted in 970 μL of 50 mM NH_4HCO_3 aqueous solution. The mixed solution was centrifuged at 14000 rpm for 25 min to remove precipitate. The supernatant was denatured at 100 °C for 5 min and then was mixed with 30 μg of trypsin to incubate at 37 °C for 20 h. Human plasma (250 μL plasma in 750 μL ultrapure water) and vortexed at 25 °C for 1 h.

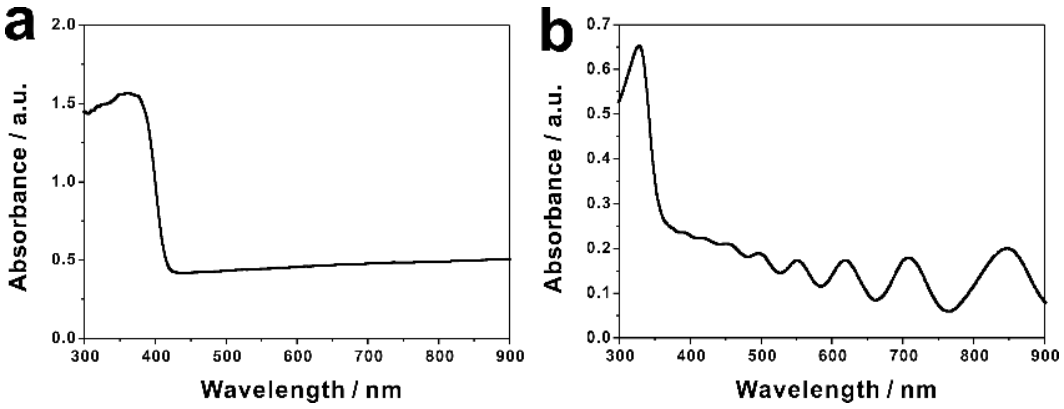

Figure S1. Diffuse reflectance spectra of absorbance of (a) r-TiO_2 NWs and (b) a-TiO_2 NTs.

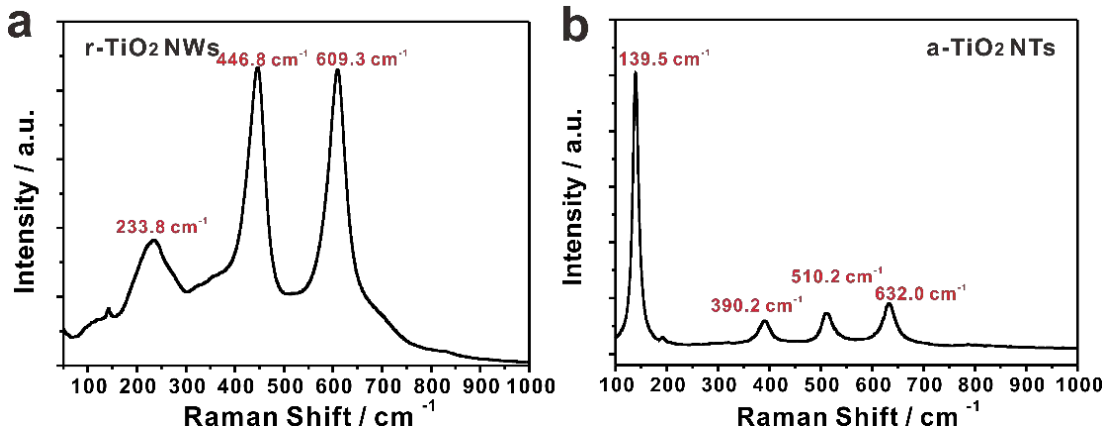

Figure S2. Raman spectra of (a) r-TiO_2 NWs and (b) a-TiO_2 NTs.

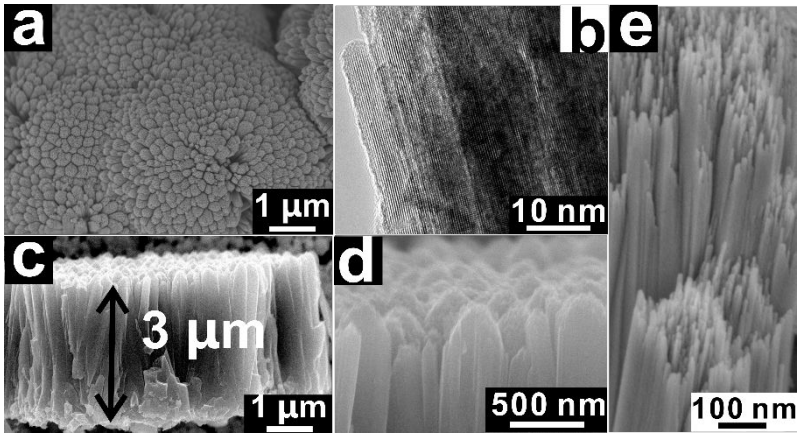

Figure S3. (a) Top-view SEM image; (b) TEM image; (c) cross-sectional SEM image; (d) high magnification of cross-sectional SEM image; (e) closer observation of high resolution of top-view SEM image.

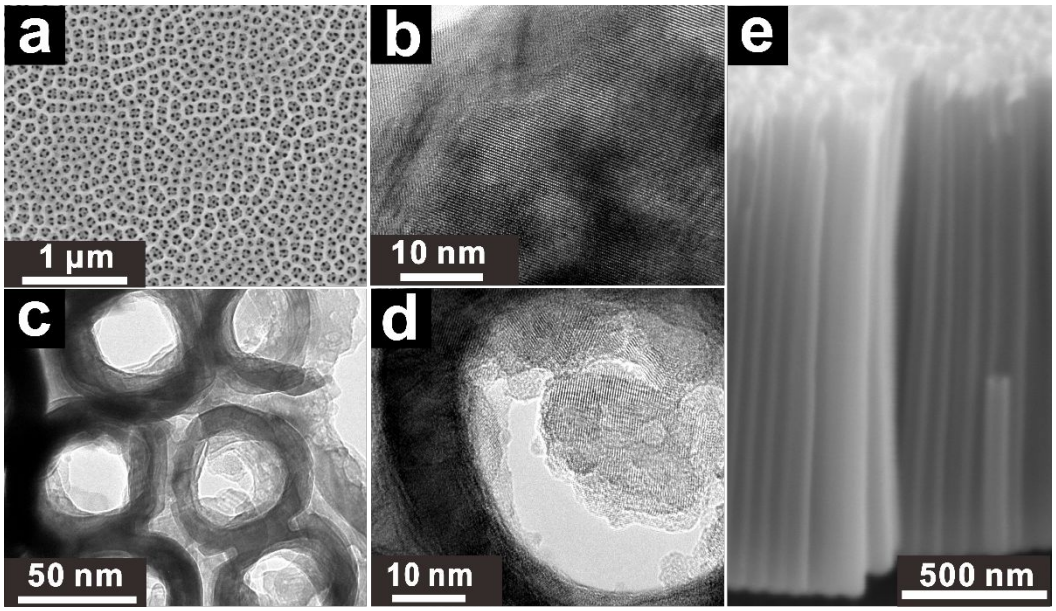

Figure S4. (a) Top-view SEM image; (b-d) TEM images; (e) cross-sectional SEM image.

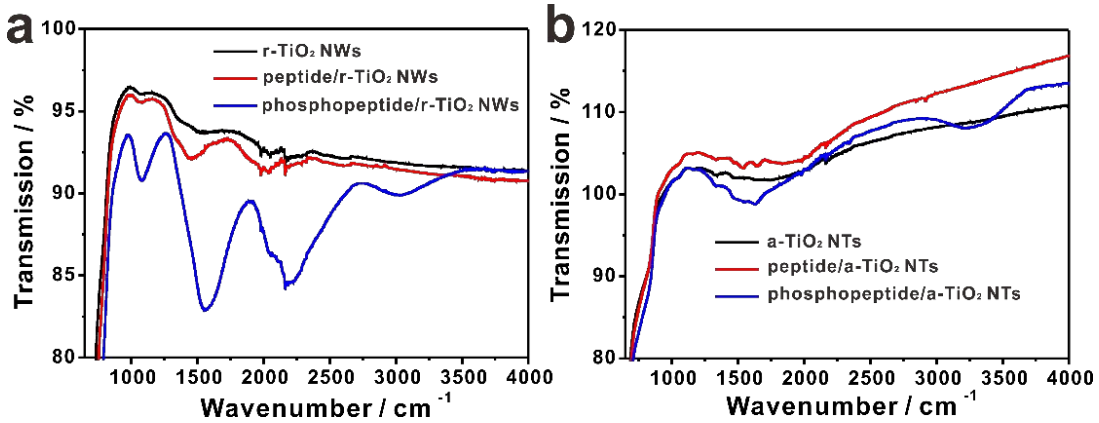

Figure S5. FTIR spectroscopy of (a) r-TiO_2 NWs, peptide/r-TiO_2 NWs, phosphopeptide/r-TiO_2 NWs; (b) a-TiO_2 NTs, peptide/a-TiO_2 NTs, phosphopeptide/a-TiO_2 NTs.

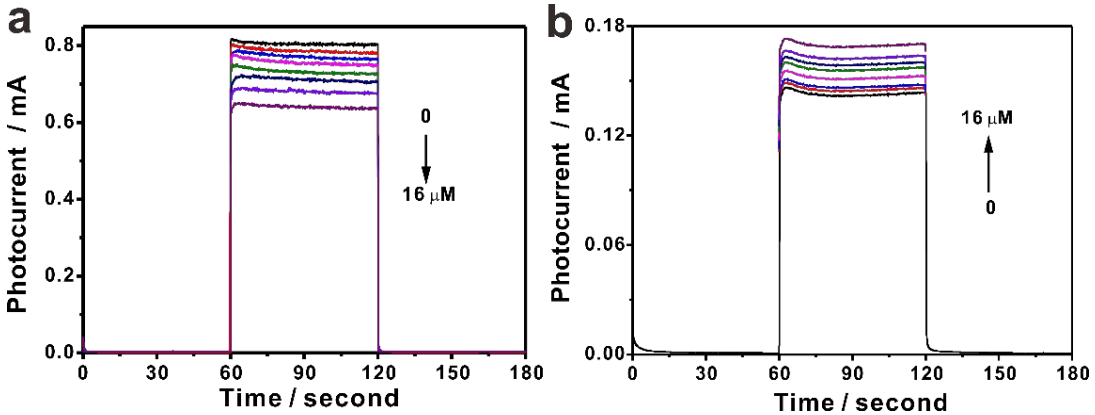

Figure S6. Amperometric transient photocurrent vs time plots of (a) r-TiO_2 NWs and (b) a-TiO_2 NTs at applied potential of 0.5 V vs Ag/AgCl under illumination of simulated solar light with different concentrations of phosphopeptides.

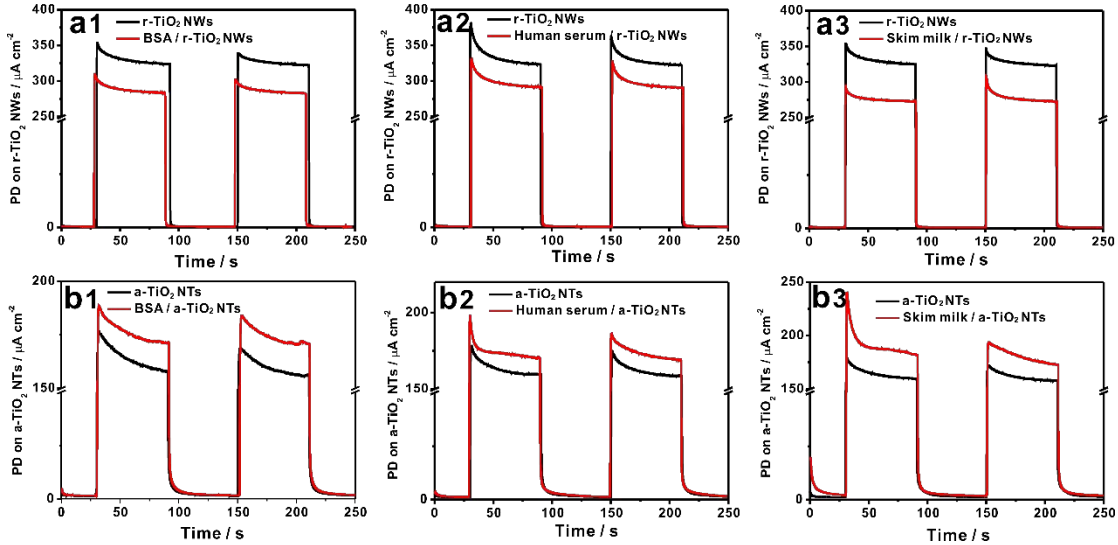

Figure S7. PEC responses of (a1) BSA, (a2) human serum, and (a3) skim milk on r-TiO_2 NWs, and of (b1) BSA, (b2) human serum, and (b3) skim milk on a-TiO_2 NTs.

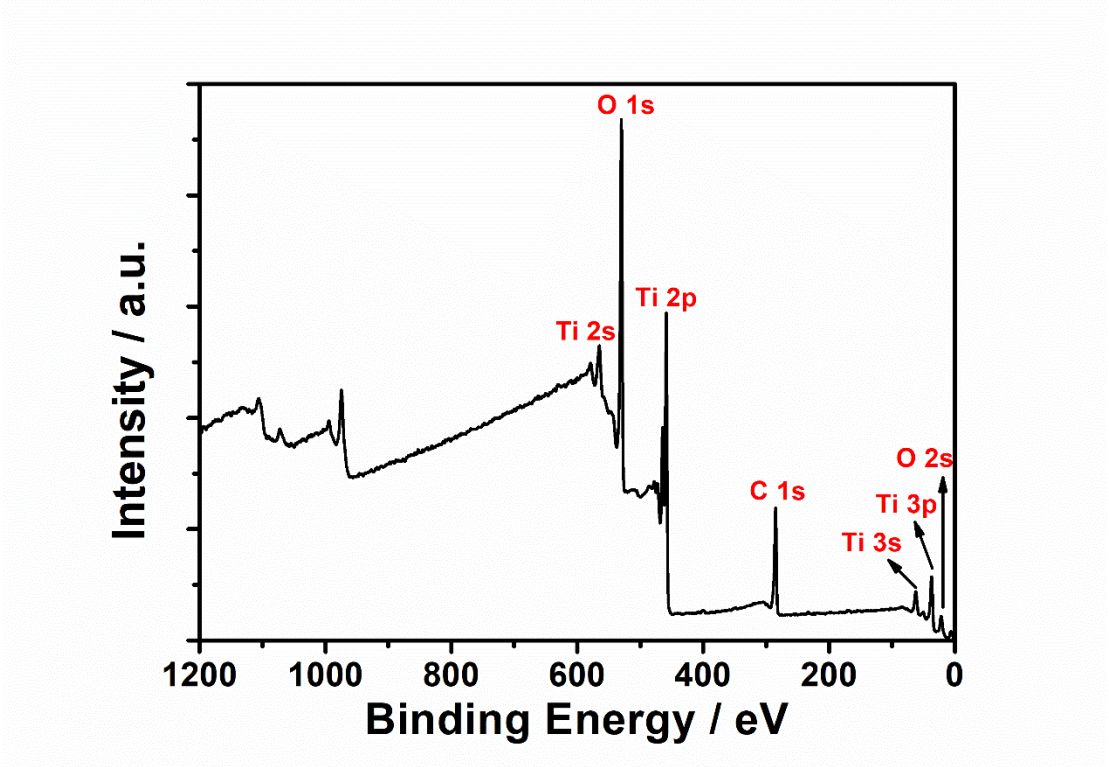

Figure S8. XPS survey of nonphosphopeptide/r-TiO_2 NWs.

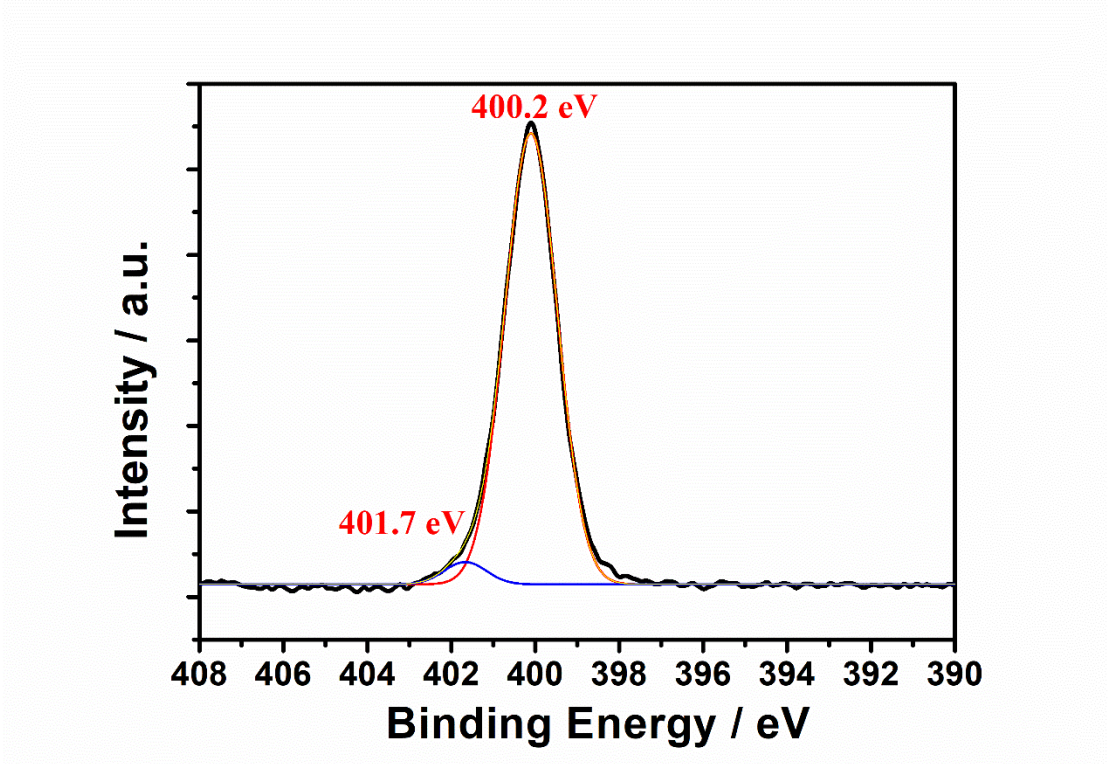

Figure S9. Core-level XPS of N 1s on phosphopeptide/r-TiO_2 NWs.

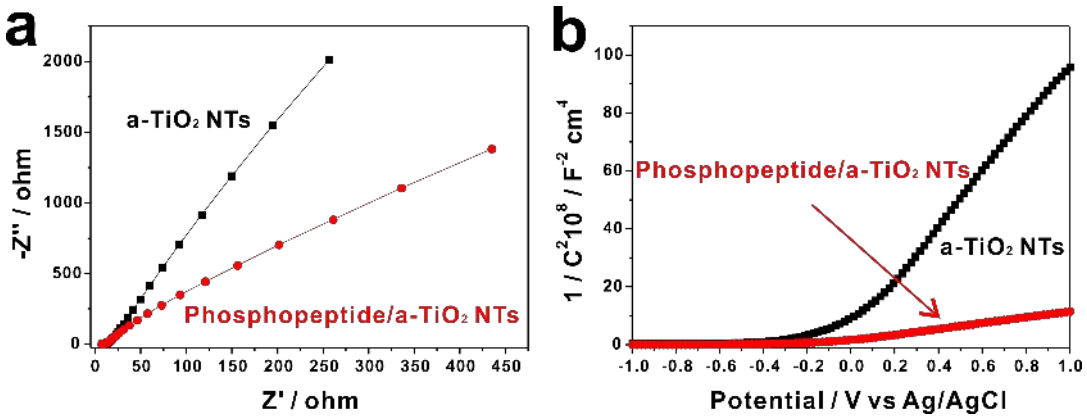

Figure S10. (a) Electrochemical impedance spectra of Nyquist plots of a-TiO_2 NTs and phosphopeptide/a-TiO_2 NTs, (b) Mott-Schottky plots of a-TiO_2 NTs and phosphopeptide/a-TiO_2 NTs.

The electrochemical impedance spectrum (EIS) is a powerful tool to study the interfacial properties of photoelectrodes. The Nyquist plots of EIS of a-TiO_2 NTs and phosphopeptide/a-TiO_2 NTs are presented in Figure S9a. After adsorption of phosphopeptides, the phosphopeptide/a-TiO_2 NTs sample showed much smaller semicircle diameter than the pristine a-TiO_2 NTs sample, indicated its smaller charge transfer resistance and faster electron mobility. In addition, the capacitance measurement on the electrode/electrolyte was also conducted to determine their carrier density (N_D) following the equation below:[1]

$$\frac{1}{C^2} = \frac{2}{N_D e \varepsilon_0 \varepsilon}\left[\left(U_S - U_{FB}\right) - \frac{k_B T}{e}\right] \qquad (1)$$

where C is the space charge capacitance in the semiconductor; N_D is the electron carrier density; e is the elemental charge value; ε_0 is the permittivity of the vacuum; ε is the relative permittivity of the semiconductor; Us is the applied potential; T is temperature; and k_B is the Boltzmann constant. The carrier density N_D was determined from the Mott-Schottky (MS) plots as $1/C^2$ *vs* potential in Figure S9b using the following equation:

$$N_D = -\left(\frac{2}{e\varepsilon\varepsilon_0}\right)\left(\frac{d(1/C^2)}{d(U_s)}\right)^{-1} \qquad (2)$$

with $e = 1.6 \times 10^{19}$, $\varepsilon_0 = 8.86\times10^{-12}$ F/m, and $\varepsilon = 48$ for anatase TiO_2[2]. The calculate donor densities are 4.9×10^{17}, and 7.5×10^{18} cm^{-3} for a-TiO_2 NTs and phosphopeptide/a-TiO_2 NTs respectively. The significantly increased N_D revealed that the phosphate anion doping improved the electrical conductivity, and thus accelerated the electron transfer.

II. Additional References

1 Wang, G.; Wang, Q.; Lu, W.; Li, J. *J. Phys. Chem. B* **2006**, *110*, 22029.
2 Ghosh, P. K.; Azimi, M. E. *IEEE Trans. Dielectr. Electr. Insul*. **1994**, *1*, 975.